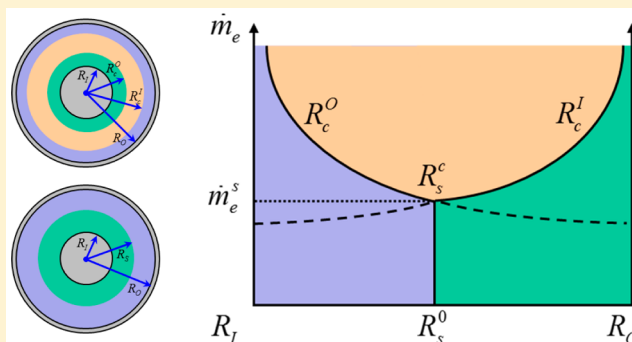


Evaporation Limited Radial Capillary Penetration in Porous Media

Mingchao Liu,[†] Jian Wu,[‡] Yixiang Gan,[§] Dorian A. H. Hanaor,[§] and C. Q. Chen^{*,†}[†]Department of Engineering Mechanics, CNMM & AML and [‡]AML & Center for Mechanics and Materials, Department of Engineering Mechanics, Tsinghua University, Beijing 100084, China[§]School of Civil Engineering, The University of Sydney, Sydney, NSW 2006, Australia

ABSTRACT: The capillary penetration of fluids in thin porous layers is of fundamental interest in nature and various industrial applications. When capillary flows occur in porous media, the extent of penetration is known to increase with the square root of time following the Lucas-Washburn law. In practice, volatile liquid evaporates at the surface of porous media, which restricts penetration to a limited region. In this work, on the basis of Darcy's law and mass conservation, a general theoretical model is developed for the evaporation-limited radial capillary penetration in porous media. The presented model predicts that evaporation decreases the rate of fluid penetration and limits it to a critical radius. Furthermore, we construct a unified phase diagram that describes the limited penetration in an annular porous medium, in which the boundaries of outward and inward liquid are predicted quantitatively. It is expected that the proposed theoretical model will advance the understanding of penetration dynamics in porous media and facilitate the design of engineered porous architectures.



1. INTRODUCTION

Capillary penetration of fluid in porous media is an important phenomenon in a broad range of applications including microfluidic devices,^{1,2} paper-based fuel cells,^{3,4} textile engineering,^{5,6} oil recovery,⁷ diagnostic testing,⁸ inkjet printing,⁹ and flow in biological tissues.¹⁰ Furthermore, dynamic wicking can also be employed to determine the effective properties (e.g., the pore size distribution and porosity) of porous media.^{11–13} Capillary penetration in porous media shares a similar dynamic mechanism with capillary flow in hollow tubes. The capillary flow of liquids in a tube or a porous medium is driven by negative capillary pressure, and porous media can be simplified as hollow tubes with an effective capillary radius.

The dynamics of capillary flow in a tube was described by Lucas¹⁴ and Washburn¹⁵ a century ago. They suggested that the distance of liquid movement L and the penetration time t satisfy a diffusion relationship as $L = (Dt)^{1/2}$, where D is the diffusion coefficient depending on the tube size and liquid properties. This classical result is valid for both horizontal and vertical capillary flow (ignoring the effect of gravity). The diffusion correlation between capillary penetration distance and time in porous media has also been found to follow the Lucas–Washburn law for both unidirectional^{16–18} and radial^{19–22} penetration, including the unidirectional capillary flow in porous media with nonuniform cross section.^{23–27}

In practical applications, volatile liquid evaporates from the surface of porous media during penetration and as a result of this continuous evaporation, the advance rate of liquid fronts is considerably diminished.²⁸ Thus, the evaporation effect will induce a limited penetration process whereby liquid penetration

is restricted to a limited region.^{28–30} Similar behavior has also been observed for vertically oriented capillary penetration with non-negligible gravitational effects.^{31–33} In order to quantitatively investigate the evaporation effect in unidirectional capillary penetration, Fries et al.²⁸ experimentally investigated the wicking of liquids into a metallic weave. The Lucas–Washburn law was employed and enhanced to model the dynamical wicking process by incorporating the effects of evaporation and gravity. They found that the evaporation of liquid at the surface has a significant effect on capillary penetration, and the penetration velocity and the maximum height are controlled by the evaporation rate. Recently, the evaporation effect has also attracted much interest in paper-based sensors and diagnostics,^{34,35} in which evaporation may restrict the penetration dynamics of the detecting reagent.

The studies discussed above focused on evaporation during unidirectional penetration, but less work has dealt such effects during radial penetration. For radial fluid penetration, which is widely applied in printing,³⁶ paper-based microfluidics and pumps,^{37,38} and textile industries,³⁹ the relationship between penetration distance and nondimensional time differs to that of the unidirectional case.²² An improved physical understanding of radial capillary penetration with evaporation will help advance the understanding penetration dynamics toward the design of porous architectures for engineering applications.

Received: June 28, 2016

Revised: August 28, 2016

Published: September 1, 2016

This Article presents the effects of evaporation on radial capillary penetration. On the basis of Darcy's law and the principle of mass conservation, a general theoretical model for evaporation-limited radial capillary penetration in homogeneous porous media is constructed. For both outward and inward radial transport, the critical radii of the limited penetration regions are determined theoretically as a function of the evaporation rate. Moreover, the limited penetration in an annular porous medium is described by a unified phase diagram to quantitatively predict the boundaries of the liquid distribution regions.

2. THEORETICAL MODEL

The radial capillary penetration of liquids into porous media is driven by the capillary force along the meniscus at the edge of the spreading spot. The process is usually described by the theoretical model given by the Lucas–Washburn law.³⁹ Here we consider a two-dimensional radial penetration of liquid into a thin porous layer with thickness much smaller than its radial dimension such that it can be treated as a planar problem in polar coordinates. If the penetration takes place from an unlimited liquid reservoir placed at the middle of the plate, the liquid flow outward along the radial direction, is termed “outward transport”; see Figure 1a. In contrast, as shown in Figure 1b, the

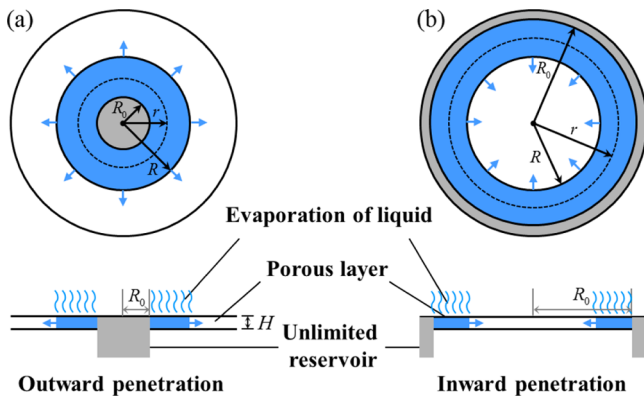


Figure 1. Schematic illustration of radial capillary penetration incorporating evaporation for (a) outward and (b) inward cases.

inward radial flow from an unlimited reservoir placed around the perimeter of a circular plate is termed “inward transport”. Both outward and inward fluid penetrations are common in paper and textile industries.^{20–22} Recently, they are also widely applied in paper-based microfluidics and pumps.^{37,38}

Consider the evaporation weakened radial capillary penetration, as shown in Figure 1, the evaporation rate \dot{m}_e , which is the mass of evaporated liquid per area and time [$\text{kg}/\text{m}^2\cdot\text{s}$], is used to characterize the evaporation of liquid. On the basis of the assumption that the evaporation rate is constant and uniform in the penetration region, the total mass flow rate due to evaporation is

$$\dot{M}_e = \dot{m}_e \cdot \pi(R^2 - R_0^2) \quad (1)$$

where R and R_0 are the radii of the wetted region and the liquid reservoir, respectively. Note that here we assume that evaporation only takes place at the top surface of the porous layer with area $\pi(R^2 - R_0^2)$. The evaporation area will be doubled if the bottom surface is also subjected to evaporation.

For a thin porous layer with thickness H and porosity ϕ , the conservation of mass during the penetration process for both inward and outward cases can be expressed as

$$2\pi r H \phi \cdot \dot{r} = 2\pi R H \phi \cdot \dot{R} + \frac{\dot{m}_e}{\rho} \cdot \pi(R^2 - r^2) \quad (2)$$

where r is the local radial position, while \dot{r} and \dot{R} are the velocities of the local position and the liquid front, respectively. Furthermore, Darcy's law for the liquid flow can be expressed as

$$\frac{Q}{A} = -\frac{K}{\mu} \frac{\partial P}{\partial r} \quad (3)$$

where Q is the flux of the liquid flow through a cylindrical surface with area $A = 2\pi r H$, K is the permeability of the porous medium, μ is the viscosity of the liquid, and P is the pressure of liquid. For radial penetration, liquid flow flux can be related to the local liquid velocity as

$$Q = i A \phi, \quad \dot{r} = \frac{dr}{dt} \quad (4)$$

Integration of eq 3 and combining with eqs 2 and 4 yield

$$P_c = \frac{\mu \phi}{k} R \ln\left(\frac{R}{R_0}\right) \frac{\partial R}{\partial t} + \frac{1}{4} \frac{\mu \dot{m}_e}{k \rho H} \left[(R_0^2 - R^2) + 2R^2 \ln\left(\frac{R}{R_0}\right) \right] \quad (5)$$

where the second term of the right-hand side refers to the viscous pressure loss P_m due to the evaporation effect and represents the resistance in the penetration process and P_c is the capillary pressure. The capillary pressure also depends on the surface tension, σ , the contact angle formed between solid and liquid, θ_s , and the effective pore radius of the porous medium, R_{eff} with the form

$$P_c = \frac{2\sigma \cos \theta_s}{R_{\text{eff}}} \quad (6)$$

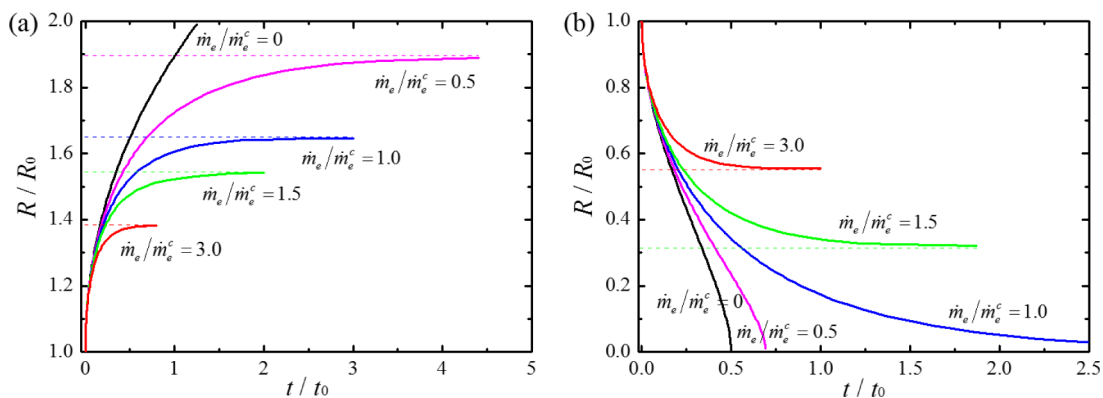


Figure 2. Normalized radii versus normalized time for (a) outward and (b) inward radial penetration of liquid under different evaporation rates. Dashed lines indicate critical penetration radii.

By substitution of the above equation into eq 5, the penetration radius can be solved as a function of time for both outward (see Figure 1a, $R > R_0$) and inward (see Figure 1b, $R < R_0$) cases.

For the limiting case of negligible evaporation, i.e., $\dot{m}_e = 0$, eq 5 reduces to the classical radial penetration model.³⁹ In eq 5, a time scale, $t_0 = \mu\phi R_0^2/2KP_c$, can be defined to normalize the penetration time.

As mentioned above, the evaporation effect acts as a resistance to the penetration process. Consequently, the liquid penetration will be restricted to a limited region with a critical radius. From eq 5, we find that the speed of liquid penetration reduces to zero (i.e., the penetration process is stopped) when the capillary pressure equals the evaporation-induced viscous pressure loss (i.e., $P_c = P_m$). Thus, the critical radius R_c depends on the evaporation rate, and can be given as

$$\left(\frac{R_c}{R_0}\right)^2 \left[1 - 2\ln\left(\frac{R_c}{R_0}\right)\right] = 1 - \frac{\dot{m}_e^c}{\dot{m}_e} \quad (7)$$

where \dot{m}_e^c is a critical evaporation rate that allows inward penetrating liquid to reach the center of the circular porous plate. By substituting $R_c \rightarrow 0$ into the equilibrium condition $P_c = P_m$, we obtain the value as $\dot{m}_e^c = 4P_c(k\rho H/\mu R_0^2)$. It is clear that this critical evaporation rate depends on the geometrical and physical parameters of the porous medium and the liquid, and can be controlled by changing these system parameters.

3. RESULTS AND DISCUSSION

3.1. Limited Outward and Inward Radial Penetration.

We first consider the evaporation effect on the radial capillary penetration in a thin porous layer. According to the developed model of eq 5, combining with the two defined parameters t_0 and \dot{m}_e^c , the normalized penetration radius of the thin porous layer, R/R_0 , can be plotted versus the normalized penetration time, t/t_0 , for outward and inward radial penetration (shown in Figure 2 for different evaporation rates).

For outward penetration, as shown in Figure 2a, R/R_0 increases with time and the speed of penetration is smaller for larger values of \dot{m}_e/\dot{m}_e^c . More interestingly, the outward penetration radius approaches an asymptote (i.e., the critical R/R_0) when the time is sufficiently long and $\dot{m}_e/\dot{m}_e^c \neq 0$. This phenomenon is the above-mentioned evaporation-limited radial penetration. It is clear that the critical radius of the limited penetration region decreases with increasing evaporation rate.

Figure 2b shows the evaporation effect for the case of inward penetration, where R/R_0 is plotted as a function of t/t_0 for five cases (i.e., $\dot{m}_e/\dot{m}_e^c = 0, 0.5, 1.0, 1.5$ and 3.0). It can be seen that inward penetration differs fundamentally from the outward case in that there exists a critical state between the limited and unlimited penetration under the condition of $\dot{m}_e = \dot{m}_e^c$. Limited penetration occurs for an evaporation rate greater than the critical value, i.e., $\dot{m}_e \geq \dot{m}_e^c$, and the critical radius is larger for larger evaporation rates. When $\dot{m}_e \leq \dot{m}_e^c$, liquid penetrates into the whole region, but the speed of penetration still depends on the evaporation rate. From these two cases we find that the evaporation of liquid has significant effect on the radial capillary penetration.

According to the above analysis, the critical radius for evaporation-limited penetration is dependent on the evaporation rate. According to eq 7, the quantitative relationships between R_c/R_0 and \dot{m}_e/\dot{m}_e^c are plotted in Figure 3 with red and blue solid lines for outward and inward penetration, respectively. For outward penetration, the critical radius monotonically decreases and approaches the radius of the liquid reservoir, R_0 , with increasing of evaporation rates. For inward penetration, the critical radius increases from zero to R_0

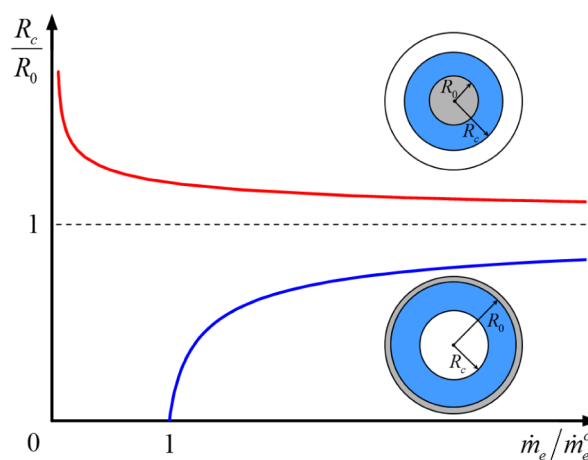


Figure 3. Normalized critical penetration radii versus normalized evaporation rate for outward and inward radial penetration.

when the evaporation rate \dot{m}_e is larger than the critical value \dot{m}_e^c . When $\dot{m}_e \leq \dot{m}_e^c$, the critical radius remains zero, which means the liquid can penetrate the entire region. Figure 3 indicates that the limited region of radial penetration can be controlled by the evaporation rate.

In the above analysis, all the results are given in a dimensionless form. In particular, the evaporation rate \dot{m}_e is normalized by a critical value \dot{m}_e^c , which is governed by material parameters and environmental conditions. The definition of the critical evaporation rate can be rearranged as

$$\dot{m}_e^c = \frac{4\sigma \cos \theta \rho}{\mu} \frac{2k}{R_{\text{eff}}} \frac{H}{R_0^2} \quad (8)$$

The expression in eq 8 consists of three parts representing the various influences on the critical evaporation rate. It is clear that \dot{m}_e^c depends on not only the properties of the liquid (i.e., surface tension, density and viscosity) and the porous medium (i.e., permeability and effective radius), but also the geometrical parameters of the porous media. Furthermore, the physical properties of liquid are affected by environmental conditions such as temperature. It means that we can control the critical evaporation rate (for instance, by changing the environmental conditions) in order to further tune the liquid penetration process.

In order to quantitatively investigate the factors affecting the critical rate of evaporation, variation of the critical evaporation rate versus the radius of the liquid reservoir is plotted in Figure 4, in which the reservoir size may represent droplet size in inkjet printing or detected reagent container in microfluidics. For comparison, two types of liquid (i.e., water and hydrofluoroether, HFE-7500), which are common used in industrial and natural applications and show significant difference of properties, under three temperature conditions, $T = 20, 50,$ and 80 °C, are considered. The layer thickness is chosen as $H = 0.1$ mm. The parameters of the porous medium are obtained from Fries et al.,²⁸ and the physical properties of water and HFE-7500 at different temperatures are retrieved from the results of Vargaftik et al.⁴⁰ and Rausch et al.,⁴¹ respectively.

Figure 4 clearly shows that the critical evaporation rate decreases as the radius of the liquid reservoir increases for both liquids. For each liquid, higher temperatures lead to higher critical evaporation rates for a given reservoir radius.

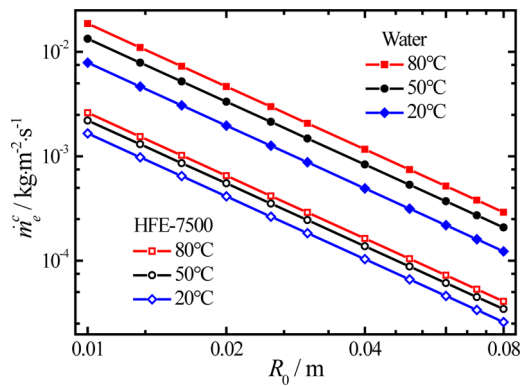


Figure 4. Comparison of the critical evaporation rate against the radius of the liquid reservoir for water and HFE-7500 under different temperatures.

Furthermore, by comparing the results of the two types of liquid, it can also be found that the critical evaporation rate of water is larger than that of HFE-7500 under the same conditions. This indicates that the evaporation relies on the penetrating liquid. Furthermore, the evaporation process will also be affected by the ambient humidity. Therefore, one can tune the liquid penetration by adopting different liquids and/or changing ambient conditions.

3.2. Limited Penetration of an Annular Porous Medium. The evaporation effect on both outward and inward fluid penetration has been investigated and we have found that there exists a critical radius depending on the evaporation rate in evaporation-limited penetration. In some practical applications of paper-based microfluidics or pumps, annular devices utilize outward and inward liquid penetrations simultaneously.^{37,38} The developed theoretical model can be applied to this type of configuration with implications in the design of microfluidic devices. Here, an annular porous medium with outer radius R_O and inner radius R_I fed by a circular reservoir in the inner boundary and ring reservoir at the outer boundary, as shown in Figure 5a, is considered. The inner and outer reservoirs contain the same liquid, which penetrates into the dry region.

It is intuitively expected that the inner liquid will intersect with the outer liquid at a certain position within the annular porous medium by capillary penetration. However, if the

penetration process is subjected to evaporation, as discussed above, the liquid penetration will be restricted to a limited region for both inward and outward cases. According to the equilibrium condition $P_c = P_m$, the critical radius of the outward penetration from the inner circular reservoir and the critical evaporation rate have the following relationship,

$$(\tilde{R}_c^O)^2 [1 - 2\ln(\tilde{R}_c^O)] = 1 - \dot{m}_e^c / \dot{m}_e \quad (9)$$

where $\tilde{R}_c^O = R_c^O / R_I$ is the normalized outward critical radius and $\dot{m}_e^c = 4P_c(k\rho H / \mu R_I^2)$ is the critical evaporation rate depending on the properties of liquid and porous medium, the inner radius and the thickness of the annular sample.

It is clear that the outward critical radius R_c^O is always larger than the inner radius of the annular porous medium R_I for any evaporation rate. At the same time, the relationship between the critical radius of the inward penetration from the outer ring reservoir (i.e., the inner boundary of the outer liquid) and the critical evaporation rate can be given as

$$(\tilde{R}_c^I)^2 [1 - 2\ln(\tilde{R}_c^I / \alpha)] = \alpha^2 - \dot{m}_e^c / \dot{m}_e \quad (10)$$

where $\tilde{R}_c^I = R_c^I / R_I$ is the normalized inward critical radius, with $R_c^I \leq R_O$ for any evaporation rate.

When the evaporation rate increases from zero to a sufficiently large value, the inner and outer liquid regions become separate. The critical state, at which the two regions start separating, can be defined by a critical evaporation rate \dot{m}_e^s and by $R_c^O = R_c^I$. Combining with eqs 9 and 10, we obtain

$$\dot{m}_e^s = \dot{m}_e^c / [1 - (\tilde{R}_c^s)^2 (1 - 2\ln \tilde{R}_c^s)] \quad (11)$$

where $\tilde{R}_c^s = R_c^s / R_I$ is the normalized radius of the separated position, which relates to the dimensionless geometric factor of the annular porous layer, $\alpha = R_O / R_I$, by

$$\tilde{R}_c^s = \sqrt{(\alpha^2 - 1) / 2\ln \alpha} \quad (12)$$

When the evaporation rate satisfies $\dot{m}_e \leq \dot{m}_e^s$, the intersected boundary between the inner and the outer liquid can be obtained by solving the following integral equation

$$\int_{R_I}^{R_s} \frac{(\mu\phi/K)R}{P_c - P_m^I} \ln \frac{R}{R_I} dR = \int_{R_O}^{R_s} \frac{(\mu\phi/K)R}{P_c - P_m^O} \ln \frac{R}{R_O} dR \quad (13)$$

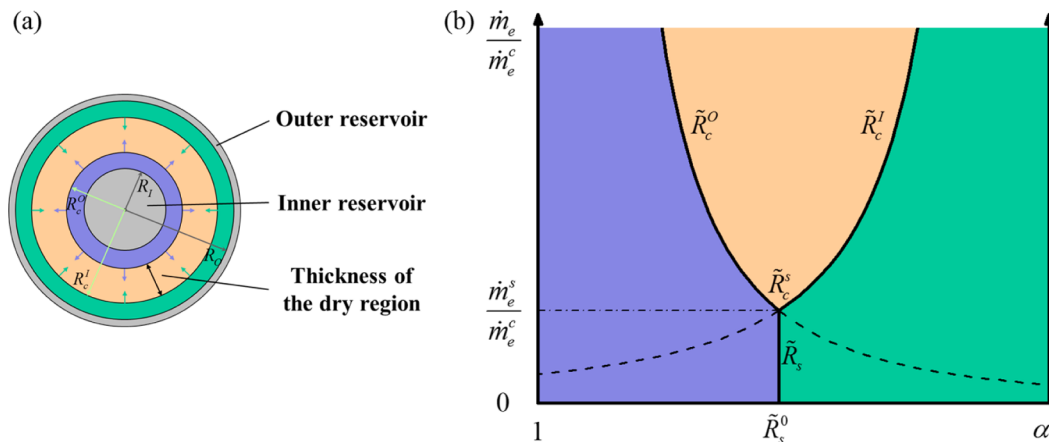


Figure 5. (a) Schematic illustration of an annular porous medium fed by inner and outer reservoirs. (b) Calculated phase diagram of evaporation limited radial capillary penetration in an annular porous medium.

Equation 13 can be simplified when the evaporation rate is negligible. The corresponding explicit solution is

$$\tilde{R}_s^0 = R_s^0/R_1 = \sqrt{(\alpha^2 - 1)/2\ln\alpha} \quad (14)$$

It is interesting to note that R_c^s and R_s^0 are found to share the same value, which depends only on the geometric parameters of the annular porous medium. However, if two different types of liquids are considered for the inner and outer reservoirs, a difference between R_c^s and R_s^0 may be observed.

Based on the above analysis, the limited penetration in an annular porous medium can be determined by two dimensionless parameters (i.e., the normalized radius of the annular, R/R_1 , and the normalized evaporation rate, \dot{m}_e/\dot{m}_e^c). Therefore, it can be described by a unified phase diagram, as shown in Figure 5b. It can be seen that the whole space is divided into three regions separated by phase boundaries (solid lines). The shaded blue and green regions describe those penetrated by the inner and outer liquid, respectively. The solid line between them shows the intersected boundary between the inner and the outer liquid and governed by eq 13, with two end points given by eqs 12 and 14. It worth noting that the abscissa remains constant, which means that the intersection boundary is not dependent on the evaporation rate. When the evaporation rate is larger than the critical value \dot{m}_e^c given by eq 11, there will be a dry region, as shown in yellow in Figure 5. The boundaries of the inner and outer fluid regions are governed by eqs 9 and 10, respectively.

Figure 5b clearly shows that evaporation limits penetration in an annular porous medium. On the basis of this unified phase diagram, we can control the liquid penetration process or design the porous structure quantitatively. When the evaporation rate is larger than the critical value \dot{m}_e^c there will be a dry gap in the annular porous medium with thickness $\Delta R_c = R_c^i - R_c^o$. In practical applications, the thickness of the dry region is a usable design parameter. For a more intuitive understanding, the normalized thickness of the dry region is plotted as a function of the normalized evaporation rate in Figure 6. It can be found that the thickness of this dry region approaches the dimensions of the gap between the inner and outer reservoirs as the evaporation rate tends to infinity.

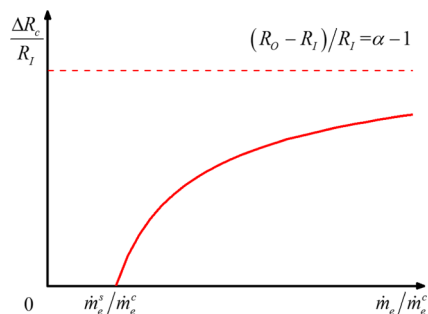


Figure 6. Variation of the normalized dry region thickness with the normalized evaporation rate.

It should be noted that in the phase diagram the evaporation rate is normalized by the critical value. As discussed, the critical evaporation rate is governed by material properties and ambient conditions. The boundaries of the phase diagram will shift in response to changes in fluid or ambient conditions. Thus, the liquid distribution in the annular sample is tunable.

4. CONCLUSION

In this work, based on Darcy's law and the principle of mass conservation, a general framework has been developed to quantitatively describe the evaporation effect on radial capillary penetration. The proposed model shows that evaporation has significant effects on radial capillary penetration in thin porous layers.

For both outward and inward radial capillary penetration, evaporation reduces the rate of liquid penetration. Furthermore, liquid penetration may be restricted to a limited region with a critical radius, which depends on the evaporation rate and the geometric parameters of the porous samples. For inward fluid penetration a critical value of the evaporation rate exists, above which limited penetration will occur. For penetration in an annular porous medium, the obtained unified phase diagram shows that the outer liquid intersects with the inner liquid when the evaporation rate is smaller than a critical value. Otherwise, a dry region exists between the outer and inner liquid penetrated regions. The phase boundaries in this diagram can be predicted theoretically.

This study provides a quantitative theoretical exploration of the evaporation-limited radial penetration in thin layer porous media. The present analysis provides a useful framework to investigate the underlying mechanisms of limited capillary penetration in environments with non-negligible evaporation, and also warrants new designs of porous architectures to optimize the capillary penetration processes for a wide range of practical applications. It should be noted that the adopted method can also be extended to the unidirectional penetration in porous media exhibiting rectangular geometries.

AUTHOR INFORMATION

Corresponding Author

*Tel/Fax: +86 10 62783488. E-mail: chenccq@tsinghua.edu.cn.

Notes

The authors declare no competing financial interest.

ACKNOWLEDGMENTS

The authors are grateful for the financial support of this work by the National Natural Science Foundation of China (No. 11472149 and 11202113) and the Tsinghua University Initiative Scientific Research Program (No. 2014z22074).

REFERENCES

- (1) Li, X.; Tian, J. F.; Shen, W. Thread as A Versatile Material for Low-Cost Microfluidic Diagnostics. *ACS Appl. Mater. Interfaces* **2010**, *2*, 1–6.
- (2) Owens, T. L.; Leisen, J.; Beckham, H. W.; Breedveld, V. Control of Microfluidic Flow in Amphiphilic Fabrics. *ACS Appl. Mater. Interfaces* **2011**, *3*, 3796–3803.
- (3) Ge, J.; Schirhagl, R.; Zare, R. N. Glucose-Driven Fuel Cell Constructed from Enzymes and Filter Paper. *J. Chem. Educ.* **2011**, *88*, 1283–1286.
- (4) Narvaez Villarrubia, C. W.; Lau, C.; Ciniciato, G. P. M. K.; Garcia, S. O.; Sibbett, S. S.; Petsez, D. N.; Babanova, S.; Gupta, G.; Atanassov, P. Practical Electricity Generation from A Paper Based Biofuel Cell Powered by Glucose in Ubiquitous Liquids. *Electrochem. Commun.* **2014**, *45*, 44–47.
- (5) Kim, E.; Xia, Y. N.; Whitesides, G. M. Polymer Microstructures Formed by Molding in Capillaries. *Nature* **1995**, *376*, 581–584.
- (6) Liu, Y. Y.; Xin, J. H.; Choi, C. H. Cotton Fabrics with Single-faced Superhydrophobicity. *Langmuir* **2012**, *28*, 17426–17434.
- (7) Morrow, N. R.; Mason, G. Recovery of Oil by Spontaneous Imbibition. *Curr. Opin. Colloid Interface Sci.* **2001**, *6*, 321–337.

- (8) Martinez, A. W.; Phillips, S. T.; Whitesides, G. M. Three-dimensional Microfluidic Devices Fabricated in Layered Paper and Tape. *Proc. Natl. Acad. Sci. U. S. A.* **2008**, *105*, 19606–19611.
- (9) Clarke, A.; Blake, T. D.; Carruthers, K.; Woodward, A. Spreading and Imbibition of Liquid Droplets on Porous Surfaces. *Langmuir* **2002**, *18*, 2980–2984.
- (10) Jeong, K. Y.; Lee, J. S.; Paik, D. H.; Jung, W. K.; Choi, S. W. Fabrication of Cell-penetrable Microfibrous Matrices with A Highly Porous Structure Using A Simple Fluidic Device for Tissue Engineering. *Mater. Lett.* **2016**, *168*, 116–120.
- (11) Marmur, A.; Cohen, R. D. Characterization of Porous Media by the Kinetics of Liquid Penetration: The Vertical Capillaries Model. *J. Colloid Interface Sci.* **1997**, *189*, 299–304.
- (12) Marmur, A. Kinetics of Penetration into Uniform Porous Media: Testing the Equivalent-capillary Concept. *Langmuir* **2003**, *19*, 5956–5959.
- (13) Fragiadaki, E.; Harhalakis, S.; Kalogianni, E. P. Characterization of Porous Media by Dynamic Wicking Combined with Image Analysis. *Colloids Surf., A* **2012**, *413*, 50–57.
- (14) Lucas, R. Rate of Capillary Ascension of Liquids. *Kolloid-Z.* **1918**, *23*, 15–22.
- (15) Washburn, E. W. The Dynamics of Capillary Flow. *Phys. Rev.* **1921**, *17*, 273–283.
- (16) Delker, T.; Pengra, D. B.; Wong, P. Z. Interface Pinning and the Dynamics of Capillary Rise in Porous Media. *Phys. Rev. Lett.* **1996**, *76*, 2902.
- (17) Lago, M.; Araujo, M. Capillary Rise in Porous Media. *J. Colloid Interface Sci.* **2001**, *234*, 35–43.
- (18) Nia, S. F.; Jessen, K. Theoretical Analysis of Capillary Rise in Porous Media. *Transp. Porous Media* **2015**, *110*, 141–155.
- (19) Marmur, A. The Radial Capillary. *J. Colloid Interface Sci.* **1988**, *124*, 301–308.
- (20) Borhan, A.; Rungta, K. K. On the Radial Spreading of Liquids in Thin Porous Substrates. *J. Colloid Interface Sci.* **1992**, *154*, 295–297.
- (21) Danino, D.; Marmur, A. Radial Capillary Penetration into Paper: Limited and Unlimited Liquid Reservoirs. *J. Colloid Interface Sci.* **1994**, *166*, 245–250.
- (22) Conrath, M.; Fries, N.; Zhang, M.; Dreyer, M. E. Radial Capillary Transport from an Infinite Reservoir. *Transp. Porous Media* **2010**, *84*, 109–132.
- (23) Mendez, S.; Fenton, E. M.; Gallegos, G. R.; Petsev, D. N.; Sibbett, S. S.; Stone, H. A.; Zhang, Y.; López, G. P. Imbibition in Porous Membranes of Complex Shape: Quasi-stationary Flow in Thin Rectangular Segments. *Langmuir* **2010**, *26*, 1380–1385.
- (24) Benner, E. M.; Petsev, D. N. Potential Flow in the Presence of a Sudden Expansion: Application to Capillary Driven Transport in Porous Media. *Phys. Rev. E* **2013**, *87*, 033008.
- (25) Shou, D.; Ye, L.; Fan, J.; Fu, K. Optimal Design of Porous Structures for the Fastest Liquid Absorption. *Langmuir* **2014**, *30*, 149–155.
- (26) Shou, D.; Ye, L.; Fan, J.; Fu, K.; Mei, M.; Wang, H.; Chen, Q. Geometry-Induced Asymmetric Capillary Flow. *Langmuir* **2014**, *30*, 5448–5454.
- (27) Shou, D.; Fan, J. Structural Optimization of Porous Media for Fast and Controlled Capillary Flows. *Phys. Rev. E* **2015**, *91*, 053021.
- (28) Fries, N.; Odic, K.; Conrath, M.; Dreyer, M. The Effect of Evaporation on The Wicking of Liquids into a Metallic Weave. *J. Colloid Interface Sci.* **2008**, *321*, 118–129.
- (29) Lockington, D. A.; Parlange, J. Y.; Lenkopane, M. Capillary Absorption in Porous Sheets and Surfaces Subject to Evaporation. *Transp. Porous Media* **2007**, *68*, 29–36.
- (30) Beyhaghi, S.; Geoffroy, S.; Prat, M.; Pillai, K. M. Wicking and Evaporation of Liquids in Porous Wicks: A Simple Analytical Approach to Optimization of Wick Design. *AIChE J.* **2014**, *60*, 1930–1940.
- (31) Fries, N.; Dreyer, M. An Analytic Solution of Capillary Rise Restrained by Gravity. *J. Colloid Interface Sci.* **2008**, *320*, 259–263.
- (32) Fries, N.; Dreyer, M. Dimensionless Scaling Methods for Capillary Rise. *J. Colloid Interface Sci.* **2009**, *338*, 514–518.
- (33) Standnes, D. C. Scaling Group for Spontaneous Imbibition Including Gravity. *Energy Fuels* **2010**, *24*, 2980–2984.
- (34) Jahanshahi-Anbuhi, S.; Henry, A.; Leung, V.; Sicard, C.; Pennings, K.; Pelton, R.; Brennan, J. D.; Filipe, C. D. Paper-based Microfluidics with An Erodible Polymeric Bridge Giving Controlled Release and Timed Flow Shutoff. *Lab Chip* **2014**, *14*, 229–236.
- (35) Liu, Z.; Hu, J.; Zhao, Y.; Qu, Z.; Xu, F. Experimental and Numerical Studies on Liquid Wicking into Filter Papers for Paper-based Diagnostics. *Appl. Therm. Eng.* **2015**, *88*, 280–287.
- (36) Kawase, T.; Siringhaus, H.; Friend, R. H.; Shimoda, T. Inkjet Printed Via-hole Interconnections and Resistors for All-polymer Transistor Circuits. *Adv. Mater.* **2001**, *13*, 1601.
- (37) Cate, D. M.; Adkins, J. A.; Mettakoonpitak, J.; Henry, C. S. Recent Developments in Paper-based Microfluidic Devices. *Anal. Chem.* **2015**, *87*, 19–41.
- (38) Wang, X.; Hagen, J. A.; Papautsky, I. Paper Pump for Passive and Programmable Transport. *Biomicrofluidics* **2013**, *7*, 014107.
- (39) Hyväluoma, J.; Raiskinmäki, P.; Jäsberg, A.; Koponen, A.; Kataja, M.; Timonen, J. Simulation of Liquid Penetration in Paper. *Phys. Rev. E* **2006**, *73*, 036705.
- (40) Vargaftik, N. B.; Vinogradov, Y. K.; Yargin, V. S. *Handbook of Physical Properties of Liquids and Gases*; Begell House: New York, 1996.
- (41) Rausch, M. H.; Kretschmer, L.; Will, S.; Leipertz, A.; Fröba, A. P. Density, Surface Tension, and Kinematic Viscosity of Hydrofluoroethers HFE-7000, HFE-7100, HFE-7200, HFE-7300, and HFE-7500. *J. Chem. Eng. Data* **2015**, *60*, 3759–3765.